



Proteomic analysis of retinopathy-related plasma biomarkers in diabetic patients

Chieh-Hsiang Lu^{a,b,1}, Szu-Ting Lin^{c,1}, Hsiu-Chuan Chou^d, Ying-Ray Lee^{e,*}, Hong-Lin Chan^{c,*}

^a Division of Endocrinology and Metabolism, Department of Internal Medicine, Chiayi Christian Hospital, Chiayi, Taiwan

^b Department of Business Administration, National Chung Cheng University, Chiayi, Taiwan

^c Institute of Bioinformatics and Structural Biology and Department of Medical Science, National Tsing Hua University, Hsinchu, Taiwan

^d Department of Applied Science, National Hsinchu University of Education, Hsinchu, Taiwan

^e Department of Medical Research, Chiayi Christian Hospital, Chiayi, Taiwan

ARTICLE INFO

Article history:

Received 21 September 2012
and in revised form 14 October 2012
Available online 4 December 2012

Keywords:

Retinopathy
Diabetes
DIGE
Proteomics

ABSTRACT

Diabetic retinopathy occurs in approximately 25% of patients with type 1 or type 2 diabetes; the disease can cause poor vision and even blindness because high glucose levels weaken retinal capillaries, causing leakage of blood into surrounding areas. We adopted a proteomics-based approach using 2D-DIGE and MALDI-TOF/TOF MS to compare the differential plasma proteome between diabetic retinopathy with significant retinopathy occurrence within 5 years after diagnosis of diabetes, and diabetic non-retinopathy without diagnosed retinopathy for more than 10 years after diagnosis of diabetes. We identified 77 plasma proteins, which represent 28 unique gene products. These proteins mainly have inflammatory response and coagulation roles. Our approach identified several potential diabetic retinopathy biomarkers including afamin and the protein arginine N-methyltransferase 5, which may be associated with the progression and development of diabetes. In conclusion, we report a comprehensive patient-based plasma proteomic approach to the identification of potential plasma biomarkers for diabetic retinopathy screening and detection.

© 2012 Elsevier Inc. All rights reserved.

Introduction

The retina is a light-sensitive nerve layer located at the back of the eye that creates images of objects. These specialized cells survive by obtaining nutrients and oxygen from tiny blood vessels in the eye. Retinopathy is a disease of the retina that occurs in approximately 25% of patients with type 1 or type 2 diabetes [1,2]. Diabetic retinopathy can cause poor vision and even blindness because high glucose levels can weaken retinal capillaries, resulting in leakage of blood into the surrounding space. This bleeding can result in formation of scar tissue, which can cause stresses in the retina, causing it to detach from the wall of the eye. The involvement of hyperglycemia in the pathogenesis of diabetic retinopathy may cause macular edema because of damage to the blood-retinal barrier. Such damage can cause blood protein leakage and consequent thickening and swelling of the macular, and eventually, distorted central vision. However, the detailed molecular processes, and the diagnostic biomarkers of the disease are not yet fully understood [3–7].

* Corresponding authors. Address: Institute of Bioinformatics and Structural Biology & Department of Medical Science, National Tsing Hua University, No. 101, Kuang-Fu Rd. Sec.2, Hsinchu 30013, Taiwan. Fax: +886 3 5715934 (H. L. Chan).

E-mail addresses: yingray.lee@gmail.com (Y.-R. Lee), hlchan@life.nthu.edu.tw (H.-L. Chan).

¹ These authors contributed equally.

Two-dimensional gel electrophoresis (2-DE) and MALDI-TOF MS have wide application in profiling plasma proteins. Nonionic and zwitterionic detergents, such as thiourea and CHAPS, can improve the solubility of plasma proteins. The introduction of fluorescent 2D-DIGE has allowed significant progress in gel-based analysis for protein quantification and detection. A single electrophoresis gel can contain numerous samples, so minimizing gel-to-gel variation. The use of an internal fluorescent standard facilitates the comparison of protein features across different gels. This innovative strategy relies on the pre-labeling of protein samples with fluorescent dyes Cy2, Cy3, and Cy5 to allow multiple experimental samples to include an internal standard. Thus, a single gel can concurrently separate multiple samples. The internal standard, which is a pool of equal aliquots of experimental protein samples, facilitates data accuracy in normalization, and increases statistical confidence in relative quantities across gels [8–12].

The development of new techniques to monitor diabetic retinopathy is essential for both diagnosis and prognosis. Proteomics is a powerful tool for the analysis of complex mixtures of proteins and the identification of biomarkers. To examine differentially expressed levels of plasma proteins that are associated with diabetic retinopathy, we used a proteomics-based approach involving a combination of immunodepletion of high abundance proteins. 2D-DIGE analysis and MALDI-TOF MS analysis to obtain a panel of plasma proteins that were differentially expressed between diabetic retinopathy cases with significant retinopathy occurrence

within 5 years following diagnosis, and diabetic non-retinopathy cases without diagnosed retinopathy within 10 years after diabetes diagnosis.

Materials and methods

Chemicals and reagents

Generic chemicals, albumin, and an IgG depletion kit were purchased from Sigma–Aldrich (St. Louis, USA). All reagents and the Cy2, Cy3, and Cy5 fluorescent dyes were purchased from GE Healthcare (Uppsala, Sweden). All chemicals used in this study were analytical grade. All primary antibodies used in this study were purchased from GeneTex (Hsinchu, Taiwan).

Cell lines and cell cultures

The ARPE-19 cell line was purchased from the American Type Culture Collection (Manassas, VA). ARPE-19 cells were maintained in Dulbecco's Modified Eagle's medium (DMEM) supplemented with 10% (v/v) fetal calf serum (FCS), L-glutamine (2 mM), streptomycin (100 µg/mL), and penicillin (100 IU/mL) (all purchased from Gibco-Invitrogen Corp., UK), and incubated at 37 °C under 5% CO₂.

For cell culturing at differential glucose concentrations, cultures were exposed to D-glucose at final concentrations of 25 and 100 mM (corresponding to 2 h after meal plasma glucose levels in controlled and uncontrolled diabetic patients, respectively [13]), and compared with control cultures exposed to 5.5 mM D-glucose (corresponding to fasting plasma glucose levels of diabetes-free people) [14,15]. To exclude the possible effects of hyperosmotic stress, we used mannitol to balance the differential glucose concentrations [16]. After a minimum of 3 weeks exposure, the monolayer cultures collected for analysis.

Plasma sample collection and purification

Between Jan and Dec 2011, nine donors were enrolled to the study from Chiayi Christian Hospital, Chiayi, Taiwan. Participants were divided into a diabetic retinopathy patient group ($n = 3$) and a diabetic non-retinopathy patient group ($n = 6$). The criteria used to assess the presence of diabetic retinopathy were based on pathological diagnosis and guidelines as proposed by the World Health Organization. Persons exhibiting significant retinopathy within 5 years of initial diagnosis of diabetes were assigned to the diabetic retinopathy group, and those without diagnosis of retinopathy for more than 10 years after diagnosis of diabetes were assigned to the diabetic non-retinopathy patients group. The Institutional Research Board approved this study, and it was conducted according to the Helsinki Declaration Principles. All participants provided written informed consent. The clinical data of patients were measured in the clinical laboratory and are summarized in Table 1.

To improve the performance of proteomic analysis of the plasma samples, albumin and immunoglobulin G were depleted from collected plasma samples using an albumin and IgG removal kit (Sigma, St. Louis, USA) in according with the manufacturer's instructions. The depleted plasma samples were precipitated by adding 1 aliquot of 100% TCA (at –20 °C) to 4 aliquots of sample, and incubated for 10 min at 4 °C. The precipitated protein was then recovered by centrifugation at 13 000 rpm for 10 min, and the resulting pellet was washed twice with ice-cold acetone. Air-dried pellets were resuspended in 2-DE lysis buffer containing 4% w/v CHAPS, 7 M urea, 2 M thiourea, 10 mM Tris–HCl, and 1 mM EDTA, at pH 8.3

Sample preparation for 2D-DIGE and gel image analysis

Sample preparation and Cy-dyes labeling for 2D-DIGE analysis were performed according to our previous reports with some mod-

Table 1

Clinical parameters of the diabetic patients with/without retinopathy participating in this investigation (values are mean ± SD). The values in this table are calculated with student's *t* test. The abbreviation used in this table: HbA1c: glycated Hemoglobin A1c; TG: triglyceride.

	T2DM patients	
	Diabetic retinopathy	Non-diabetic retinopathy
<i>Clinical characteristics and demographic data of the study subjects</i>		
Number (case)	3	6
Age (years)	54.67 ± 4.93	63.33 ± 8.41
Sex (M/F)	3/0	4/2
Total cholesterol (mg/dL)	200 ± 5.66	176.33 ± 33.56
Creatinine (mg/dL)	2.3 ± 1.98	1.25 ± 0.212
HbA1c (%)	11.45 ± 0.78	8.72 ± 2.27
TG (mg/dL)	91.5 ± 23.34	139.33 ± 94.48

ifications [17,18]. Briefly, plasma protein pellets were dissolved in 2-DE lysis buffer, and protein concentrations were determined using coomassie protein assay reagent (BioRad). Before performing 2D-DIGE, plasma samples from three diabetic retinopathy patients and six diabetic non-retinopathy patients were individually pooled. Protein samples (100 µg) from all participants were minimally labeled with Cy3 or Cy5 fluorescent dyes (250 pmol) at lysine residues for triplicate comparison on three 2-DE gels. To facilitate image matching and cross-gel statistical comparison, a pool of all samples was also prepared and labeled with Cy2 at a molar ratio of 2.5 pmol Cy2 per 1 µg of protein as an internal standard for all gels. Thus, the triplicate samples and the internal standard could be run and quantified over multiple 2-DE gels. The detailed procedures for fluorescence dye-labeling, isoelectric focusing electrophoresis, two-dimensional electrophoresis, and fluorescence image detection and analysis were described in our previous publication [9]. Spots displayed in all nine gel images (three images per gel) with a ≥1.5-fold or greater average increase or decrease in abundance. A *p*-value < 0.05 was considered significant for protein identification.

Protein staining, in-gel digestion, and MALDI-TOF MS analysis

Colloidal coomassie blue G-250 staining was used to visualize CyDye-labeled protein features in 2-DE gels followed by excised post-stained gel sections for identification by MALDI-TOF MS. The detailed procedures for protein staining, in-gel digestion, and MALDI-TOF MS analysis, together with the algorithm used for data processing were described in our previous publication [9]. The spectrometer was calibrated with a peptide calibration standard (Bruker Daltonics) and internal calibration was performed using the trypsin autolysis peaks at m/z 842.51 and m/z 2211.10. Peaks in the mass range of m/z 700–3000 were used to generate a peptide mass fingerprint that was searched against in the Swiss-Prot/TrEMBL database (released on 2011_08) with 531473 entries, using Mascot software v2.3.02 (Matrix Science, London, UK). We used the following strings for the search: *Homo sapiens*; tryptic digest with a maximum of one missed cleavage; carbamidomethylation of cysteine, partial protein N-terminal acetylation, partial methionine oxidation, and partial modification of glutamine to pyroglutamate and a mass tolerance of 50 ppm. Identification was accepted based on significant Mascot Mowse scores ($p < 0.05$), spectrum annotation, and observed versus expected molecular weight and *pI* on 2-DE gels.

Immunoblotting analysis and ELISA analysis

Immunoblotting and ELISA analyses were used to validate the differential abundance of proteins identified by mass spectrometry.

try. The detailed experimental procedures were described in our previous reports [17–19]. All primary antibodies used for expression validation were purchased from Genetex (Hsinchu, Taiwan). Plasma samples used for immunoblotting and ELISA analysis were not used to remove albumin and IgG because the analytical tools used were sufficiently sensitive to detect low-abundance proteins in whole plasma.

Results

2D-DIGE and mass spectrometry analyses of the immunodepleted plasma proteome

Immunoglobulin G and albumin account for 70–80% plasma proteins, and these high abundance fractions are an obstacle to proteomic analysis and protein biomarker discovery. Removing the high abundance immunoglobulin G and albumin from plasma samples can increase the visibility of low-abundance proteins, and facilitate the accuracy of quantitative analysis. The depleted plasma used in this study had significantly reduced levels of serum albumin, and both light- and heavy-immunoglobulin G chains (Fig. 1).

To study changes to the plasma proteome in diabetic retinopathy patients, we performed comparative proteomic analysis between the diabetic retinopathy and non-retinopathy groups. Plasma samples from the two groups were minimally labeled with Cy3 and Cy5 dyes and distributed to each 2-DE gel. A pool of both

samples was labeled with Cy2 as an internal standard to run on all gels, to facilitate image matching across gels (Fig. 2).

The plasma sample arrangement for a triplicate fluorescent 2D-DIGE experiment is shown in Fig. 2A. The triplicate samples, resolved in separate 2-DE gels, were quantitatively analyzed by reference to the internal standard present on each 2-DE gel. After resolving the plasma protein samples, the student's *t*-test, carried out using DeCyder image analysis software, revealed 207 proteins with greater than a 1.5-fold change in expression level ($p < 0.05$). MALDI-TOF MS identification revealed that 77 proteins, corresponding to 28 unique proteins, were differentially expressed (Fig. 2B, Fig. 3, and Table 2). Most of the identified proteins are functionally involved in inflammatory response (22%) and coagulation (37%), and 91% of the differentially expressed proteins identified were secreted proteins (Fig. 4).

Representative examples for evaluation of alterations in fluorescence 2D-DIGE spot intensities using Decyder software are shown in Fig. 5. To illustrate alterations in spot intensities, selected spots (haptoglobin, vitronectin, serum amyloid P-component, and leucine-rich alpha-2-glycoprotein) are represented as 3-D images, together with the associated graph views of standardized abundances of the selected spots and spot locations (Fig. 5).

Validation by immunoblotting and ELISA

To verify the abundances of proteins identified by 2D-DIGE and MALDI-TOF/TOF MS, the abundance levels of identified vitronectin,

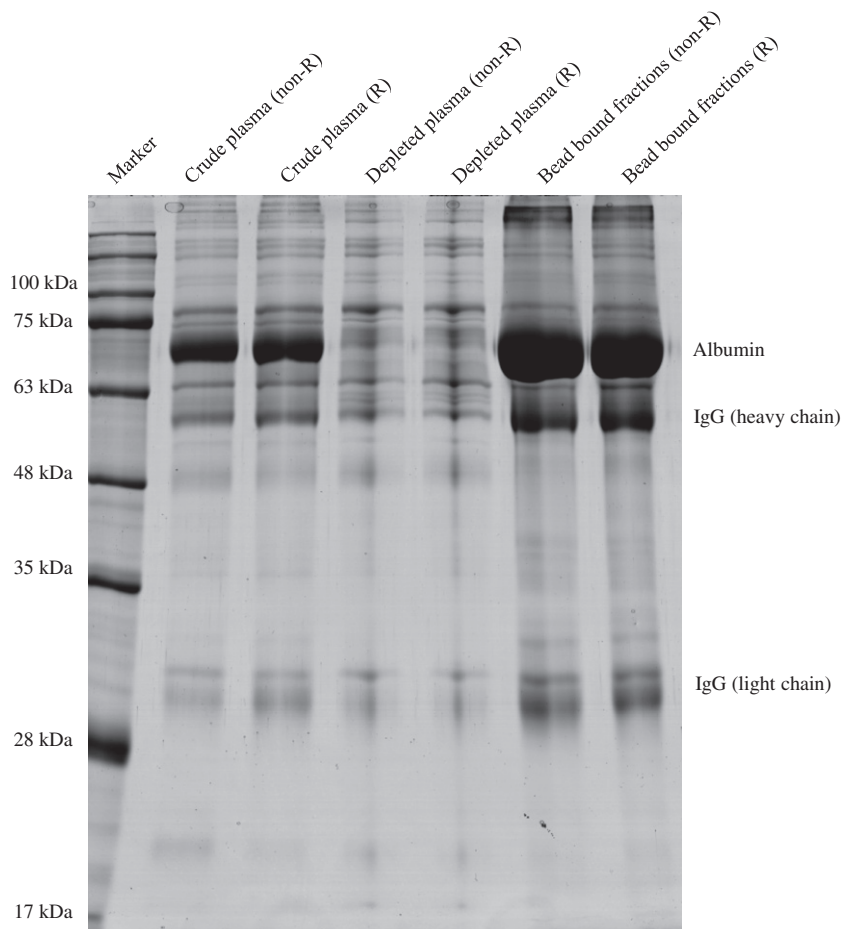


Fig. 1. Evaluation of albumin and immunoglobulin G removal efficiency from plasma samples. Twenty microgram quantities of the crude plasma, albumin, immunoglobulin-depleted plasma, and bead-bound protein fractions from diabetic patients with or without retinopathy were loaded and resolved by SDS-PAGE followed by staining with colloidal coomassie blue G-250. Non-R and R indicate diabetic non-retinopathy and retinopathy, respectively.

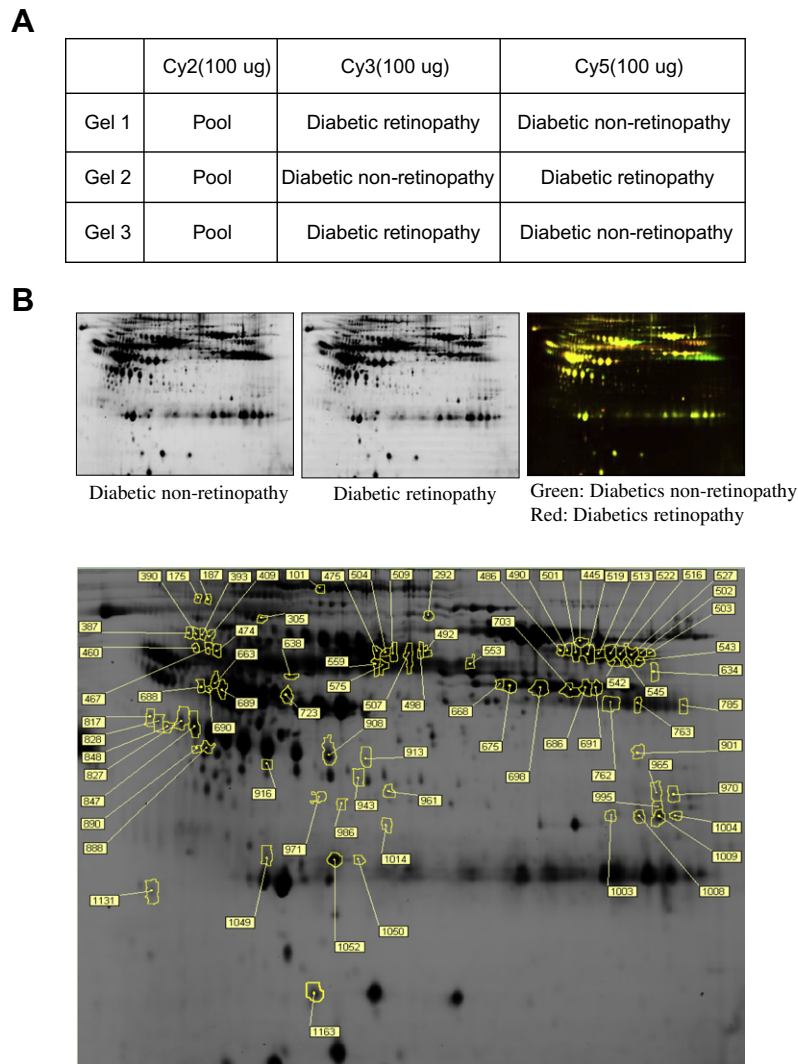


Fig. 2. 2D-DIGE analysis of retinopathy-related differentially expressed proteins. (A) Plasma sample arrangement for a triplicate 2D-DIGE experiment. (B) Plasma samples (100 µg) were labeled with Cy-fluorescent dyes, and were separated using 24 cm, pH 3–10 non-linear IPG strips. The figure shows 2D-DIGE images of the plasma samples from diabetic patients with or without retinopathy at appropriate excitation and emission wavelengths (upper left and middle images). Also shown is an overlaid pseudo-colored image processed with ImageQuant software (GE Healthcare) (upper right image). Differentially expressed protein features are annotated with spot numbers (bottom image).

leucine-rich alpha-2-glycoprotein, gelsolin, haptoglobin, and serum amyloid P-component were investigated by immunoblotting and ELISA. As shown in Fig. 6A and B, the 38 kDa leucine-rich alpha-2-glycoprotein, the 46 kDa haptoglobin and the 25 kDa serum amyloid P-component were significantly increased in the plasma of diabetic retinopathy patients compared to those levels in diabetic non-retinopathy patients. In contrast, vitronectin and gelsolin levels were significantly lower in the diabetic retinopathy plasma group. Our immunoblotting and ELISA results are consistent with data from the 2D-DIGE and MALDI-TOF/TOF MS observations, and further suggest that the identified proteins are potential markers for the diagnosis of diabetic retinopathy.

Glucose modulates cytokeratin 8, gelsolin, and leucine-rich alpha-2-glycoprotein expression in retinal epithelial cell lines

To examine whether glucose induces expression of the identified retinal proteins, we cultured retinal epithelial cell line ARPE-19 in glucose (5.5 mM, 25 mM, and 100 mM) for a minimum of

3 weeks. The expression levels of proteins cytokeratin 8, gelsolin, and leucine-rich alpha-2-glycoprotein were monitored by immunoblotting. The results demonstrated that glucose treatment augmented the amount of cytokeratin 8 and leucine-rich alpha-2-glycoprotein in ARPE-19. However, gelsolin was significantly down-regulated in high glucose cultured ARPE-19 cells (Fig. 7).

Discussion

Proteomic analysis of disease usually involve a comparative strategy that is defined by the differential expression of the associated proteins under different disease conditions. Our combined fluorescent 2D-DIGE based quantitative proteomic and MALDI-TOF analyses revealed 77 instances of altered expression in plasma proteins corresponding to 28 unique plasma proteins (Table 2). The majority of altered proteins belong to two major functional groups, inflammatory responses proteins, and coagulation proteins (Fig. 4). Of the proteins shown in Table 1, alpha, beta, and gamma plasma fibrinogen isoforms, antithrombin-III, alpha-1-antitrypsin, hipto-

Table 2
Alphabetical list of differentially expressed plasma proteins between diabetic patients with / without retinopathy as identified by MALDI-TOF MS after 2D-DIGE analysis.

NO.	Swiss-prot No.	protein name	Mw	p I	No. Match peptides	cov. (%)	score	retinopathy / non-retinopathy ^a	T-test	subcellular location	Functional classification	Selected matched peptides
305	P43652	Afamin	70963	5.64	8/15	12%	106/56	-1.72	0.037	Secreted	Transport	YSDASDCHGEDSQAFCEK HPDLSIPELLR
634	Q86U18	Alpha-1-antitrypsin	46878	5.37	14/56	40%	167/56	-1.52	0.011	Secreted	Inflammatory response	LYHSEAFVNFNGDTEEAK VFSNGADLSGVTEEAPLK
663	Q86U18	Alpha-1-antitrypsin	46878	5.37	7/10	13%	96/56	1.77	0.00011	Secreted	Inflammatory response	FLEDVKK FLENEDRR
689	Q86U18	Alpha-1-antitrypsin	46878	5.37	15/41	33%	171/56	1.54	0.015	Secreted	Inflammatory response	SASLHLPK TDTSHHDQDHPFNK
690	Q86U18	Alpha-1-antitrypsin	46878	5.37	15/41	40%	184/56	2.63	0.00017	Secreted	Inflammatory response	VFSNGADLSGVTEEAPLK DTEEDFFHVDQVTTVK FLEDVKK FLENEDR
762	Q86U18	Alpha-1-antitrypsin	46878	5.37	10/23	22%	108/56	-2.97	6.60E-05	Secreted	Inflammatory response	FLEDVKK FLENEDR
961	Q86U18	Alpha-1-antitrypsin	46878	5.37	12/46	30%	92/56	-2.23	7.60E-05	Secreted	Inflammatory response	VFSNGADLSGVTEEAPLK DTEEDFFHVDQVTTVK
101	P01023	Alpha-2-macroglobulin	164613	6.03	11/20	9%	99/56	1.69	0.0071	Secreted	Protease inhibitor	LHTEAQIQEEGTVELTGR YSDASDCHGEDSQAFCEK
638	Q9UC78	Antithrombin-III	53025	6.32	9/39	18%	81/56	1.54	0.00069	Secreted	Coagulation	FATTFYQHLADSK EVPLNTIIFMGR
1049	P02647	Apolipoprotein A-I	30759	5.56	8/26	29%	115/56	2.02	0.0093	Secreted	Transport	DYVVSQFEGSALGK AKPALEDLR
986	P02649	Apolipoprotein E	36246	5.65	6/16	17%	86/56	-2.78	0.0001	Secreted	Transport	LGPLVEQGR LQAEAFQAR
490	P35523	Chloride channel protein 1	109583	5.68	6/10	5%	56/56	2.6	0.0035	Plasma membrane	membrane potential stabilization	TGSSSTVDSK MEQSRSQQR
187	Q9UCV3	Complement C1s subcomponent	78174	4.86	6/19	8%	69/56	2.05	0.0031	Secreted	Inflammatory response	VEDPESTLFGSVIR TNFDNDIALVR
445	P01024	Complement C3	188569	6.02	8/12	6%	68/56	-2.66	0.00059	Secreted	Inflammatory response	LVAYYTLIGASGQR IPIDGSGEVLSR
890	P01024	Complement C3	188569	6.02	15/56	9%	87/56	1.53	0.0027	Secreted	Inflammatory response	VHQQYFNVELIQPQAVK ENEGFTVTAEGK
486	P02671	Fibrinogen alpha chain	95656	5.70	11/29	16%	125/56	3.02	0.00033	Secreted	Coagulation	NPSSAGSWNSGSSGPGSTGNR ESSSHHPGIAEFPGR
501	P02671	Fibrinogen alpha chain	95656	5.70	12/34	16%	105/56	2.55	0.00078	Secreted	Coagulation	GDFSSANNR GGSTSYGTGSETESPR
502	P02671	Fibrinogen alpha chain	95656	5.70	19/46	22%	127/56	1.69	0.0023	Secreted	Coagulation	GGSTSYGTGSETESPR HRPDDEAAFFDFASTGK
503	P02671	Fibrinogen alpha chain	95656	5.70	9/21	12%	70/56	1.76	0.0021	Secreted	Coagulation	NPSSAGSWNSGSSGPGSTGNR HRHPDDEAAFFDFASTGK
513	P02671	Fibrinogen alpha chain	95656	5.70	17/22	18%	225/56	2.12	0.0018	Secreted	Coagulation	GDFSSANNR ESSSHHPGIAEFPGR
516	P02671	Fibrinogen alpha chain	95656	5.70	20/61	22%	154/56	1.83	0.0027	Secreted	Coagulation	NPSSAGSWNSGSSGPGSTGNR HPDDEAAFFDFASTGK
519	P02671	Fibrinogen alpha chain	95656	5.70	22/36	31%	166/56	2.43	0.00069	Secreted	Coagulation	HRHPDDEAAFFDFASTGK SRIEVLK
522	P02671	Fibrinogen alpha chain	95656	5.70	15/38	19%	138/56	2.01	0.002	Secreted	Coagulation	NPSSAGSWNSGSSGPGSTGNR DSHSLTTNIMEILR
527	P02671	Fibrinogen alpha chain	95656	5.70	14/23	15%	172/56	1.72	0.0049	Secreted	Coagulation	GLIDEVNDQFTNR QHLPLIK
542	P02671	Fibrinogen alpha chain	95656	5.70	10/47	14%	81/56	1.72	0.0046	Secreted	Coagulation	DSDWPFCSDEDWNYK GGSTSYGTGSETESPR
543	P02671	Fibrinogen alpha chain	95656	5.70	10/44	12%	74/56	2.05	0.0029	Secreted	Coagulation	QHLPLIK VQHIQLLQK
545	P02671	Fibrinogen alpha chain	95656	5.70	8/16	12%	101/56	1.82	0.0032	Secreted	Coagulation	GLIDEVNDQFTNR HPDDEAAFFDFASTGK
965	P02671	Fibrinogen alpha chain	95656	5.70	10/42	10%	82/56	1.54	0.0099	Secreted	Coagulation	GLIDEVNDQFTNR GGSTSYGTGSETESPR
970	P02671	Fibrinogen alpha chain	95656	5.70	10/26	11%	97/56	1.6	0.0039	Secreted	Coagulation	DSDWPFCSDEDWNYK GDFSSANNR
995	P02671	Fibrinogen alpha chain	95656	5.70	8/34	8%	58/56	1.6	0.0089	Secreted	Coagulation	GLIDEVNDQFTNR GGSTSYGTGSETESPR
1003	P02671	Fibrinogen alpha chain	95656	5.70	8/25	10%	81/56	1.65	0.01	Secreted	Coagulation	GLIDEVNDQFTNR GGSTSYGTGSETESPR
1004	P02671	Fibrinogen alpha chain	95656	5.70	17/39	17%	95/56	1.69	0.0059	Secreted	Coagulation	NPSSAGSWNSGSSGPGSTGNR EVDLKDYEQQK
1008	P02671	Fibrinogen alpha chain	95656	5.70	8/18	10%	92/56	1.83	0.0033	Secreted	Coagulation	GLIDEVNDQFTNR GGSTSYGTGSETESPR
1009	P02671	Fibrinogen alpha chain	95656	5.70	9/28	10%	90/56	1.84	0.0039	Secreted	Coagulation	GLIDEVNDQFTNR GDFSSANNR
1050	P02671	Fibrinogen alpha chain	95656	5.70	24/70	29%	138/56	1.77	0.0022	Secreted	Coagulation	GDSTFESK DCDDVLQTHPSGTQSGIFNIK
1014	P02671	Fibrinogen alpha chain	95656	5.70	12/25	16%	146/56	-2.69	0.00056	Secreted	Coagulation	GLIDEVNDQFTNR NPSSAGSWNSGSSGPGSTGNR
668	P02675	Fibrinogen beta chain	56577	8.54	12/26	29%	118/56	1.78	0.0058	Secreted	Coagulation	EEAPSLRPAPPISGGGYR SILENLR
675	P02675	Fibrinogen beta chain	56577	8.54	20/48	44%	219/56	1.67	0.00021	Secreted	Coagulation	EEAPSLRPAPPISGGGYR TPCTVSCNIPVVSGK
686	P02675	Fibrinogen beta chain	56577	8.54	15/32	32%	170/56	1.52	0.0012	Secreted	Coagulation	EEAPSLRPAPPISGGGYR AHYGGFTVQNEANK
691	P02675	Fibrinogen beta chain	56577	8.54	14/29	27%	130/56	1.55	0.0019	Secreted	Coagulation	AHYGGFTVQNEANK DNDGWLTSDDPR

Table 2 (continued)

NO.	Swiss-prot No.	protein name	Mw	p I	No. Match peptides	cov. (%)	score	retinopathy / non-retinopathy ^a	T-test	subcellular location	Functional classification	Selected matched peptides
698	P02675	Fibrinogen beta chain	56577	8.54	11/39	15%	103/56	1.69	3.20E-05	Secreted	Coagulation	ECEEIIR GHRPLDK
703	P02675	Fibrinogen beta chain	56577	8.54	21/61	44%	199/56	1.91	1.20E-05	Secreted	Coagulation	EEAPSLRPAPPISGGGYR HQLYIDETVNSNIPTNLR
292	P06396	Gelsolin	86043	5.90	9/27	10%	91/56	-2.15	0.00012	Secreted	Cytoskeleton	GASQAGAPQGR SEDCFILDHGK
827	P00738	Haptoglobin	45861	6.13	9/25	21%	124/56	1.67	0.0025	Secreted	Inflammatory response	DIAPTLTYVGK SCAVAEYGVYVK
847	P00738	Haptoglobin	45861	6.13	11/28	27%	150/56	1.74	0.0031	Secreted	Inflammatory response	YVMLPVADQDQCIR ILGGHLDKAK
908	P00738	Haptoglobin	45861	6.13	8/14	18%	124/56	-1.87	0.00056	Secreted	Inflammatory response	QLVEIEK VGYVSGWGR
916	P00738	Haptoglobin	45861	6.13	13/34	33%	185/56	1.56	0.0012	Secreted	Inflammatory response	DIAPTLTYVGK YVMLPVADQDQCIR
1163	P00738	Haptoglobin	45861	6.13	6/11	9%	78/56	-1.89	0.0034	Secreted	Inflammatory response	TEGDGVYTLNDKK KQWINK
575	P01876	Ig alpha-1 chain C region	38486	6.08	7/14	21%	113/56	1.56	0.00038	Secreted	Immune response	DASGVTFTWTPSSGK YLTWASR
559	P01876	Ig alpha-1 chain C region	38486	6.08	7/27	24%	90/56	1.54	0.001	Secreted	Immune response	WLQGSQELPR SAVQGPPEP
785	P01857	Ig gamma-1 chain C	36596	8.46	8/39	36%	103/56	-4.12	1.50E-05	Secreted	Immune response	THTPCPPAPELLGGPSVFLFPPKPK TTPPVLDSDGSFFLYSK
553	P01857	Ig gamma-1 chain C region	36596	8.46	8/27	30%	89/56	1.73	0.038	Secreted	Immune response	EPQVYTLPPSR STSGGTAALGCLVK
763	P01857	Ig gamma-1 chain C region	36596	8.46	5/16	18%	76/56	-3.17	8.2E-05	Secreted	Immune response	FNWYVDGVEVHNAK GPSVFPLAPSSK
913	P01857	Ig gamma-1 chain C region	36596	8.46	9/25	28%	91/56	-1.96	0.00019	Secreted	Immune response	DTLMISR EPQVYTLPPSR
901	Q9NX62	Inositol monophosphatase 3	38828	6.38	4/5	8%	62/56	1.54	0.037	Cytoplasm	Signal transduction	KLPDLEK MFYLLK
688	Q6GMY0	Keratin, type II cytoskeletal 8	53671	5.52	5/7	8%	59/56	1.54	0.0044	Cytoplasm	Cytoskeleton	TQEKEQIK ISSSSFSR
460	P01042	Kininogen-1	72996	6.34	8/29	10%	67/56	1.55	0.013	Secreted	Protease inhibitor	EGDCPVQSGK DVFQPPPTK
467	P01042	Kininogen-1	72996	6.34	7/8	8%	98/56	1.62	0.0015	Secreted	Protease inhibitor	DFVQPPPTK ICVGCPR
474	P01042	Kininogen-1	72996	6.34	9/15	12%	108/56	1.58	0.0015	Secreted	Protease inhibitor	IASFQNCIDIYPGK RPPGFSPFR
817	P02750	Leucine-rich alpha-2-glycoprotein	38382	6.45	7/16	17%	102/56	1.88	0.0075	Secreted	Inflammatory response	GPLQLER VAAGAFQGLR
828	P02750	Leucine-rich alpha-2-glycoprotein	38382	6.45	6/17	14%	86/56	1.85	0.0062	Secreted	Inflammatory response	ALGHLDLSG NR DLLLPQPD LR
848	P02750	Leucine-rich alpha-2-glycoprotein	38382	6.45	7/21	20%	102/56	1.68	0.002	Secreted	Inflammatory response	TLDLGENQLETLPPDLLR ALGHLDLSG NR
1131	Q15154	Pericentriolar material 1 protein	230046	4.95	11/32	5%	57/56	1.54	0.048	Cytoplasm	centrosome assembly	INFSDLDQRSIGSDSQGR LPEMEPLVPR
409	O14744	Protein arginine N-methyltransferase 5	73322	5.88	6/10	7%	67/56	-1.77	0.00028	Cytoplasm	Metabolism	DWNTLIVGK KGFPVLSK
175	Q8IXT5	RNA-binding protein 12B	118372	6.34	9/16	7%	65/56	1.63	0.00086	Nucleus	Gene expression	HHDRNRNGDAIVK DLNDRPVGPR
475	Q9P157	Serum albumin	71317	5.92	22/71	27%	141/56	-1.72	6.90E-06	Secreted	Transport	AEFAEVSK LVNEVTEFAK
492	Q9P157	Serum albumin	71317	5.92	7/15	13%	110/56	-4.18	0.00016	Secreted	Transport	VFDEFKPLVEEPQNLK RPCFSALEVDETYVPK
498	Q9P157	Serum albumin	71317	5.92	13/56	19%	109/56	-3.81	0.0067	Secreted	Transport	LVNEVTEFAK NECFLQHK
504	Q9P157	Serum albumin	71317	5.92	21/47	32%	179/56	-1.87	0.014	Secreted	Transport	FQNALLVR CCTESLVNR
507	Q9P157	Serum albumin	71317	5.92	16/35	28%	197/56	-3.9	5.70E-05	Secreted	Transport	VFDEFKPLVEEPQNLK YICENQDSISSK
509	Q9P157	Serum albumin	71317	5.92	6/10	7%	78/56	-3.16	7.90E-06	Secreted	Transport	SLHTLFGDK LCTVATLR
1052	P02743	Serum amyloid P-component	25485	6.10	6/22	21%	77/56	2.5	0.00034	Secreted	Innate immunity	IVLQEQDSYGGK QGYFVEAQPK
723	P02774	Vitamin D-binding protein	54526	5.40	17/49	54%	229/56	-1.85	0.0063	Secreted	Transport	EVVSLTEACCAEGADPPCYDTR SCESNSPPVHPGTAECCCK
387	P04004	Vitronectin	55069	5.55	7/18	13%	81/56	-1.74	7.60E-05	Secreted	Cell adhesion	FEDGVLDPDYPYR VDTVDPYPYR
390	P04004	Vitronectin	55069	5.55	9/28	18%	88/56	-1.93	2.70E-05	Secreted	Cell adhesion	DVWGIEGPIDAAAFTR SIAQYWLGCAPAGHL
393	P04004	Vitronectin	55069	5.55	7/19	15%	85/56	-2.04	3.60E-05	Secreted	Cell adhesion	DWHGVPGQVDAAMAGR FEDGVLDPDYPYR
888	P25311	Zinc-alpha-2-glycoprotein	34465	5.71	12/36	40%	174/56	1.69	0.00079	Secreted	Lipid degradation	QDPPSVVVTS HQAPG EK IDVHWTR

^a Averaged differences between triplicate samples run on different gels show plasma protein abundance ratios for diabetic patients with retinopathy versus diabetic patients without retinopathy. Proteins are shown as 1.5-fold differences either up- or down-regulated ($p < 0.05$). Spots in the images are listed in the table inset. Functions were assigned according to the Swiss-Prot database entries and our literature search results.

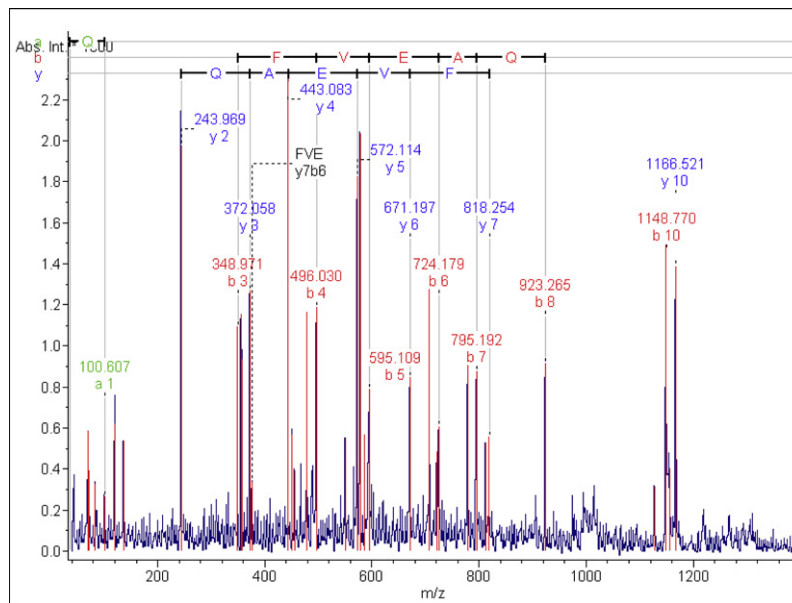
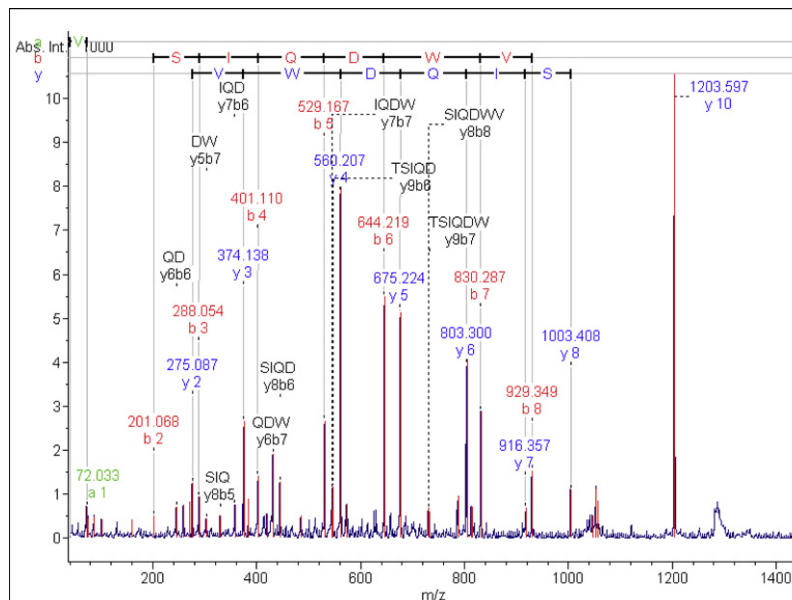
A Spot no.1052 Serum amyloid P-component**B** Spot no.847 Haptoglobin

Fig. 3. Protein identification by MALDI-TOF/TOF sequence analysis. (A) serum amyloid P-component and (B) haptoglobin were resolved by MALDI- TOF/TOF MS.

globin, complement C1/C3, and serum amyloid P-component have been previously reported as diabetic retinopathy markers [20–29]. By contrast, to the best of our knowledge, leucine-rich alpha-2-glycoprotein has not been reported as a diabetic retinopathy marker. Other functional groups of identified proteins involve plasma protein transport, and include afamin, apolipoprotein A-I, apolipoprotein E, and vitamin D-binding protein. Of these, apolipoprotein A-I and apolipoprotein E have been reported as diabetic retinopathy markers [30–33], while afamin and vitamin D-binding protein have not. Additionally, vitronectin, alpha-2-macroglobulin, and kininogen-1 have been evidenced as diabetic retinopathy markers [34–39]; but gelsolin, cytokeratin 8, and protein arginine N-methyltransferase 5 have not. Further literature searching revealed that combinations of these identified proteins have not yet been

described as diabetic retinopathy markers for other types of diabetes. Accordingly, we evaluated the combination of these identified proteins as diabetic retinopathy specific markers.

Leucine-rich alpha-2-glycoprotein has been shown to be involved in cell adhesion and to be a disease biomarker for ovarian cancer, microbial infections, non-small cell lung cancer, and pancreatic cancer [40–42]. We report for the first time that leucine-rich alpha-2-glycoprotein is a plasma biomarker for diabetic retinopathy.

Vitamin D-binding protein is a secreted protein that transports vitamin D derived sterols in serum and prevents actin polymerization. In clinical studies, vitamin D-binding protein has been widely used as a disease biomarker for breast cancer, thyroid cancer, and lung cancer [43–46]. In diabetic studies, the down-regulation

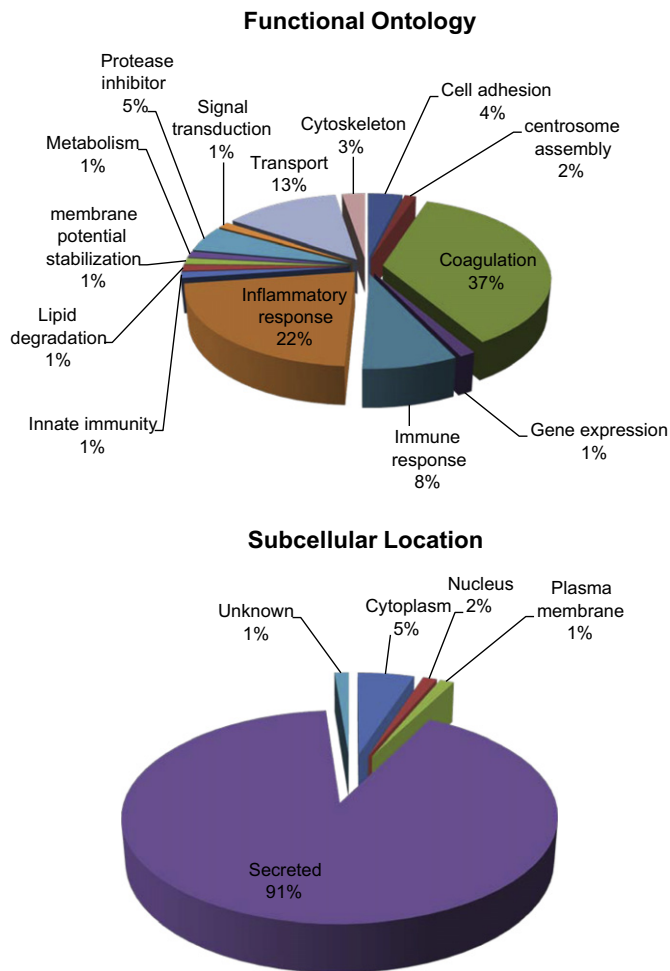


Fig. 4. Percentage of plasma proteins identified from albumin and immunoglobulin G depleted plasma by 2D-DIGE/MALDI-TOF MS for diabetic patients with or without retinopathy, according to (A) biological function and (B) subcellular location.

of vitamin D-binding protein has been associated with the progression of type 1 diabetes [47,48]. However, there is no direct evidence that links vitamin D-binding protein with diabetic retinopathy.

Afamin, a vitamin E-binding protein, has been reported as an ovary [49,50] and cervix [51] cancer marker. However, there is no report of any relationship between afamin and diabetes or diabetic retinopathy. In this proteomic study, afamin was down-regulated, implying a decreased ability to remove reactive oxygen species from the body because of the circulatory system's reduced ability to transport vitamin E.

Gelsolin is a critical regulator for actin filament assembly and disassembly; it has been identified as a novel invasion modulator in many cancers, including pancreatic cancer, bladder cancer, lung cancer, and breast cancer [52–55]. Additionally, gelsolin inhibits apoptosis by stabilizing the mitochondria [56]. Thus, the down-regulation of gelsolin for our 2D-DIGE analysis resulted in the inhibition of retinal cell growth in diabetic retinopathy.

The isolation of low-abundance plasma proteins is often difficult because of the presence of high abundance proteins such as

immunoglobulin G and serum albumin. These are the first and second most abundant proteins in plasma respectively, and constitute 70–80% of total plasma protein content. These two proteins can mask the presence of low-abundance proteins, and restrict the numbers of total plasma proteins that can be applied to proteomic analysis. We removed these proteins using an albumin and IgG depletion kit, obtained from Sigma–Aldrich, which contains pre-packed spin columns for removal of most of the immunoglobulin G and serum albumin that is present in plasma. A solution of trichloroacetic acid and acetone was used to precipitate, desalt, and enrich the plasma proteins to improve their 2D-DIGE resolution. Our results demonstrated that this strategy effectively removed most of the serum albumin, and significantly reduced the amount of immunoglobulin G that was present in samples.

Diabetic retinopathy can cause poor vision and even blindness because high glucose levels can weaken retinal capillaries leading to leakage of blood into the surrounding space, and cause distorted central vision. The modulation of glucose levels is one of the most important physiological changes in diabetic retinopathy patients. Hence, we stimulated ARPE-19 retinal epithelial cells with high glucose levels, and monitored the effect on expression of the identified proteins. The results reveal that glucose treatment regulated cytokeratin 8, gelsolin, and leucine-rich alpha-2-glycoprotein protein in both *in vivo* and *in vitro* samples (Fig. 7). We postulate that cytokeratin 8, gelsolin, and leucine-rich alpha-2-glycoprotein are important regulators and are protein signatures of the pathophysiology of diabetic retinopathy. Further investigation is necessary to elucidate the mechanistic roles of these proteins in the onset of diabetic retinopathy.

Fluorescence-based protein quantification is generally able to detect sub-nanogram quantities of dye-labeled proteins in a 2D-DIGE experiment; however, our post-staining experiment used modified colloidal coomassie blue staining, which can detect 20–50 nanogram quantities [10]. Thus, while numerous differentially expressed dye-labeled, low-abundance plasma proteins may be detected by fluorescence scanning, they can fail to be visualized with colloidal coomassie blue staining. This is the reason that only 128 out of 207 differentially expressed features were identified from the 2-DE gels for MALDI-TOF study. Furthermore, the plasma proteins are largely modified with glycans in the body's circulatory system. The high levels of glycosylated plasma proteins have been reported to interfere with trypsin digestion and with MALDI-TOF MS analysis [57]. Accordingly, glycosylation of plasma proteins might contribute to a failure in the identification of some proteins in this study.

Of the protein isoforms resolved and identified by 2D-DIGE and MALDI-TOF MS, lysine labeling identified alpha-1-antitrypsin, complement C3, and haptoglobin as doublet spots with differing *pI* values. Notably, the more basic spots (spots 634/762 in alpha-1-antitrypsin, spot 445 in complement C3, and spots 908/961/1163 in haptoglobin) in the doublet were shown to be down-regulated, while the more acidic spots (spots 663/689/690 in alpha-1-antitrypsin, spot 890 in complement C3, and spots 908/961/1163 in haptoglobin) were up-regulated. A similar observation has been reported [58,59] and was found to result from oxidation of the active site cysteine thiols of these proteins. Such shifts provide an explanation for our observation that alpha-1-antitrypsin, complement C3, and haptoglobin modified by the oxidation of thiol cysteine residues, or by glycosylation of these proteins, induce *pI* shifts in the differential labels. We further validated this model using 2D-immunoblotting to reveal that molecular modifications on alpha-1-antitrypsin, complement C3, and haptoglobin may affect protein activity. This interaction warrants further investigation.

In our plasma proteomic analysis, we used lysine labeled Cy-dyes to quantify differences in plasma protein levels between type

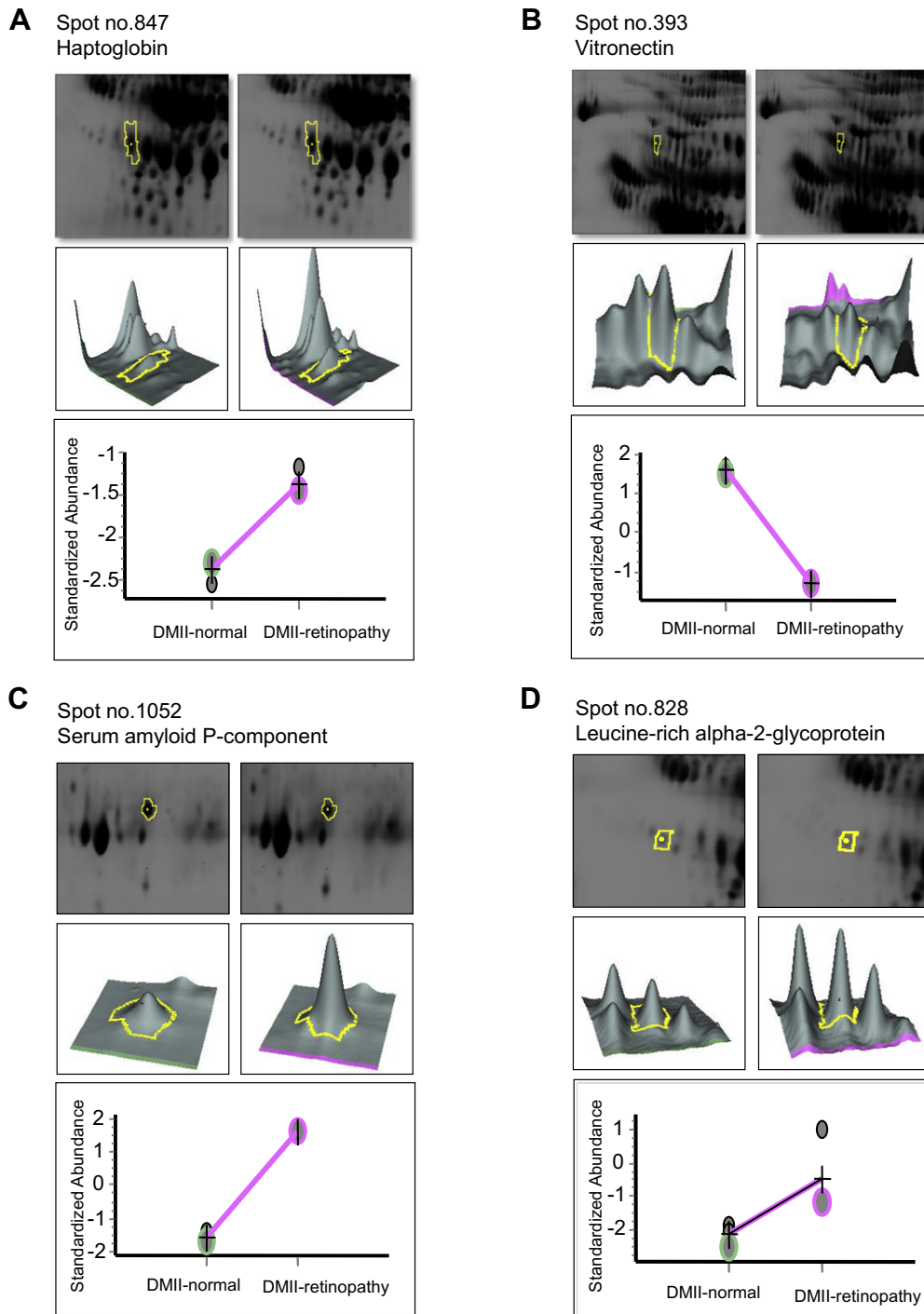


Fig. 5. Representative images of the identified protein spots (A) haptoglobin; (B) vitronectin; (C) serum amyloid P-component; (D) leucine-rich alpha-2-glycoprotein displaying changes in diabetic retinopathy-dependent protein abundance. The levels of these proteins were visualized by fluorescence 2-DE images (top panels), three-dimensional spot images (middle panels), and protein abundance mapping (lower panels).

2 diabetes patients with and without retinopathy complications. We employed a minimal labeling protocol because lysine modification might strongly interfere with the following in-gel digestion step. By contrast, a cysteine labeling protocol is suitable for monitoring oxidative stress and glycation-induced thiol reactive changes to cysteine residues. We previously reported the use of a cysteine labeling protocol to monitor cellular redox-signaling and redox-regulation of plasma proteins [10,60–62].

Due to the source of plasma samples, Our plasma samples were necessarily collected after 10-years without the develop-

ment of retinopathy complications following initial diagnosis of type 2 diabetes. Additionally, we required 5 years to confirm that plasma proteins sourced from type 2 diabetes patients were obtained in the presence of retinopathy complications. Thus, the sample size was small for this study. Notably, disease markers obtained in this study are concentrated on retinopathy specific markers in diabetic patients. It is necessary to compare plasma between healthy and diabetic donors of similar ages, to be sure of identifying type 2 diabetes associated markers.

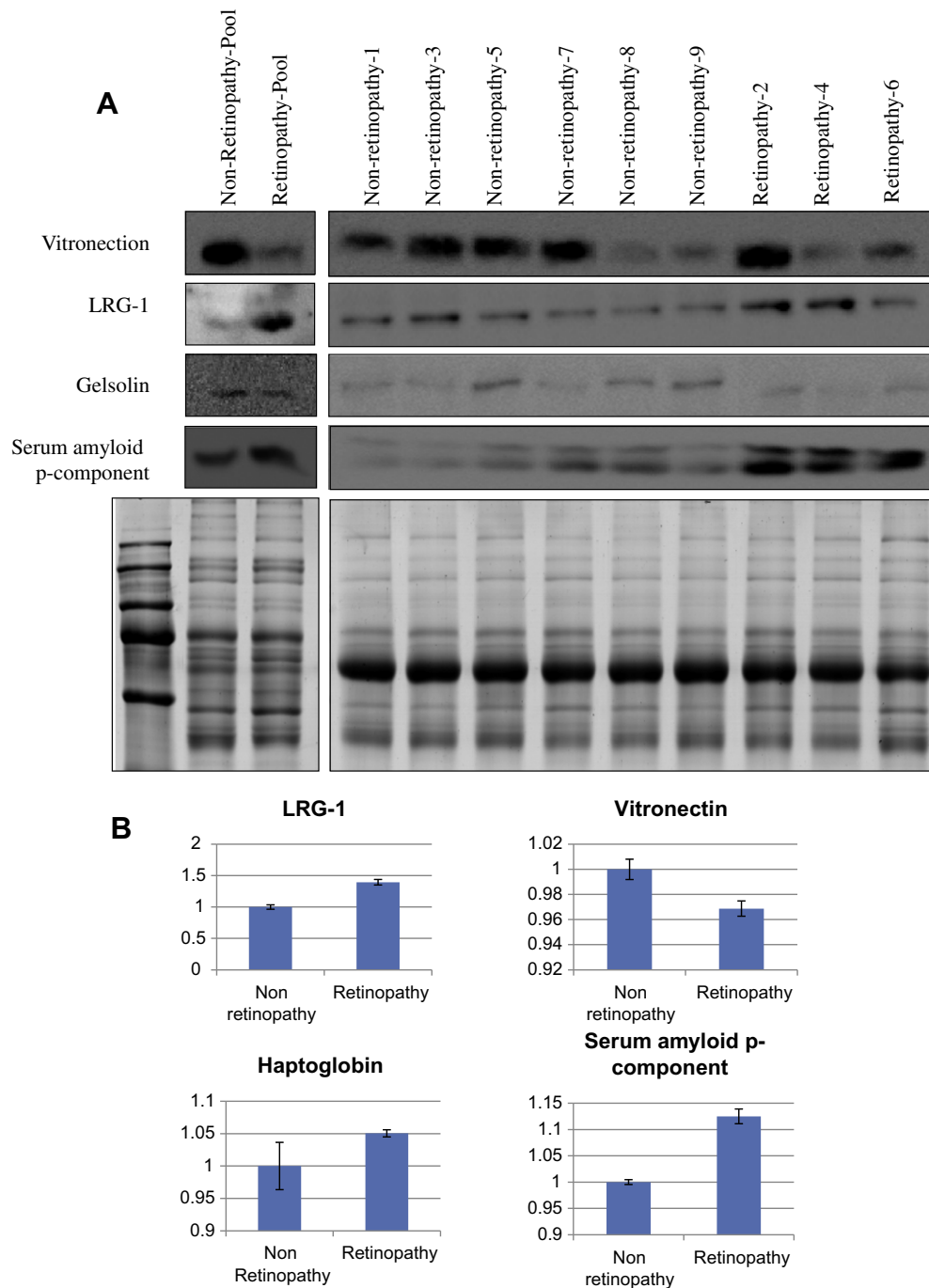


Fig. 6. Representative immunoblotting analysis of vitronectin, leucine-rich alpha-2-glycoprotein, gelsolin, and serum amyloid P-component, and ELISA analysis of leucine-rich alpha-2-glycoprotein, vitronectin, haptoglobin, and serum amyloid P-component for selected differentially expressed plasma proteins identified by proteomic analysis in diabetic patients with or without retinopathy. Plasma samples from 3 diabetic retinopathy patients and 6 diabetic non-retinopathy patients were either run individually or run in a pool. (A) 20 μ g of the albumin and immunoglobulin-depleted plasma were loaded and resolved by SDS-PAGE followed by immunoblotting with vitronectin, leucine-rich alpha-2-glycoprotein, gelsolin, and serum amyloid P-component, or stained with colloidal coomassie blue G-250 as an internal loading control. (B) 50 μ g of plasma samples were coated onto each well of a 96-well plate for ELISA analysis of leucine-rich alpha-2-glycoprotein, vitronectin, haptoglobin, and serum amyloid P-component and the absorbance measured at 450 nm using a Stat Fax 2100 microtiter plate reader.

In conclusion, our 2D-DIGE and MALDI-TOF MS based quantitative plasma proteomics analysis provided valuable information for diabetic retinopathy research. Our approach allowed us to identify 12 proteins that were previously reported as plasma markers of diabetic retinopathy. Additionally, we have presented several putative diabetic retinopathy biomarkers, including leucine-rich alpha-2-glycoprotein, afamin, vitamin D-binding protein, gelsolin, cyto-keratin 8, and arginine N-methyltransferase 5 for the progression

and development of type 2 diabetes, and may have application as a tool for monitoring the course of the disease. These marker's potential for screening and treatment of diabetic retinopathy warrants further investigation.

Declaration of competing interest

The authors confirm that there are no conflicts of interest.

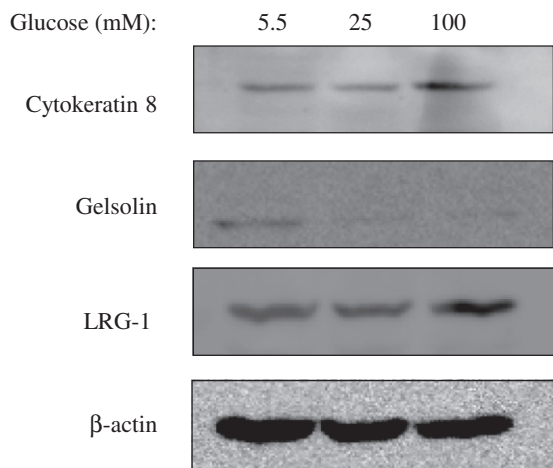


Fig. 7. Effect of glucose concentration on cytokeratin 8, gelsolin, and leucine-rich alpha-2-glycoprotein expression in cultured ARPE-19 cells. Cytokeratin 8, gelsolin, and leucine-rich alpha-2-glycoprotein expression assays were performed on ARPE-19 cells following 3 weeks incubation at different glucose concentrations (5.5 mM, 25 mM, and 100 mM glucose). Protein expression was monitored by immunoblotting against cytokeratin 8, gelsolin, and leucine-rich alpha-2-glycoprotein antibodies.

Acknowledgments

This work was supported by NSC grant (100-2311-B-007-005) from the National Science Council, Taiwan, and grant from National Tsing Hua University for Nano- and Micro- ElectroMechanical Systems-based Frontier Research on Cancer Mechanism, Diagnosis, and Treatment. The authors also thank the Chiayi Christian Hospital, Chiayi, Taiwan for grant number R101-18).

References

- [1] H. Dorchy, D. Toussaint, *Rev. Med. Brux.* 5 (1984) 319–331.
- [2] D.M. van Reyk, M.C. Gillies, M.J. Davies, *Redox. Rep.* 8 (2003) 187–192.
- [3] A.W. Stitt, *Invest Ophthalmol. Vis. Sci.* 51 (2010) 4867–4874.
- [4] F. Gelissen, F. Ziemssen, *Ophthalmologe* 107 (2010) 773–786.
- [5] R. Ehrlich, A. Harris, T.A. Ciulla, N. Kheradiya, D.M. Winston, B. Wirosko, *Acta Ophthalmol.* 88 (2010) 279–291.
- [6] T.N. Crawford, D.V. Alfaro III, J.B. Kerrison, E.P. Jablon, *Curr. Diabetes Rev.* 5 (2009) 8–13.
- [7] A. Girach, H. Lund-Andersen, *Int. J. Clin. Pract.* 61 (2007) 88–97.
- [8] H.L. Huang, H.W. Hsing, T.C. Lai, Y.W. Chen, T.R. Lee, H.T. Chan, P.C. Lyu, C.L. Wu, Y.C. Lu, S.T. Lin, C.W. Lin, C.H. Lai, H.T. Chang, H.C. Chou, H.L. Chan, *J. Biomed. Sci.* 17 (2010) 36.
- [9] T.C. Lai, H.C. Chou, Y.W. Chen, T.R. Lee, H.T. Chan, H.H. Shen, W.T. Lee, S.T. Lin, Y.C. Lu, C.L. Wu, H.L. Chan, *J. Proteome Res.* 9 (2010) 1302–1322.
- [10] H.L. Chan, S. Gharbi, P.R. Gaffney, R. Cramer, M.D. Waterfield, J.F. Timms, *Proteomics* 5 (2005) 2908–2926.
- [11] Y.W. Chen, H.C. Chou, P.C. Lyu, H.S. Yin, F.L. Huang, W.S. Chang, C.Y. Fan, I.F. Tu, T.C. Lai, S.T. Lin, Y.C. Lu, C.L. Wu, S.H. Huang, H.L. Chan, *Funct. Integr. Genomics* (2011).
- [12] H.C. Chou, Y.W. Chen, T.R. Lee, F.S. Wu, H.T. Chan, P.C. Lyu, J.F. Timms, H.L. Chan, *Free Radic. Biol. Med.* 49 (2010) 96–108.
- [13] H. Candiloros, S. Muller, N. Zeghari, M. Donner, P. Drouin, O. Ziegler, *Diabetes Care* 18 (1995) 549–551.
- [14] S.H. Saydah, M. Miret, J. Sung, C. Varas, D. Gause, F.L. Brancati, *Diabetes Care* 24 (2001) 1397–1402.
- [15] X. Jouven, R.N. Lemaitre, T.D. Rea, N. Sotoodehnia, J.P. Empana, D.S. Siscovick, *Eur. Heart J.* 26 (2005) 2142–2147.
- [16] L. Cai, W. Li, G. Wang, L. Guo, Y. Jiang, Y.J. Kang, *Diabetes* 51 (2002) 1938–1948.
- [17] P.H. Hung, Y.W. Chen, K.C. Cheng, H.C. Chou, P.C. Lyu, Y.C. Lu, Y.R. Lee, C.T. Wu, H.L. Chan, *Mol. Biosyst.* 7 (2011) 1990–1998.
- [18] Y.W. Chen, J.Y. Liu, S.T. Lin, J.M. Li, S.H. Huang, J.Y. Chen, J.Y. Wu, C.C. Kuo, C.L. Wu, Y.C. Lu, Y.H. Chen, C.Y. Fan, P.C. Huang, C.H. Law, P.C. Lyu, H.C. Chou, H.L. Chan, *Mol. Biosyst.* (2011).
- [19] C.P. Lin, Y.W. Chen, W.H. Liu, H.C. Chou, Y.P. Chang, S.T. Lin, J.M. Li, S.F. Jian, Y.R. Lee, H.L. Chan, *Mol. Biosyst.* (2011).
- [20] H. Asakawa, K. Tokunaga, F. Kawakami, *J. Diabetes Complications* 14 (2000) 121–126.

- [21] A. Sobol, *Acta Haematol. Pol.* 26 (1995) 57–62.
- [22] T.M. Davis, J.C. Moore, R.C. Turner, *Diabete Metab.* 11 (1985) 147–151.
- [23] M. Fukuda, *Eye Ear Nose Throat Mon.* 51 (1972) 266–272.
- [24] G.E. Elder, E.E. Mayne, J.G. Daly, A.L. Kennedy, D.R. Hadden, D.A. Montgomery, J.A. Weaver, *Haemostasis* 9 (1980) 288–296.
- [25] A. Matysik, J. Toczolowski, B. Jakubowska-Solarska, J. Solski, M. Lewandowska-Furmanik, *Ann. Univ. Mariae. Curie Sklodowska Med.* 57 (2002) 204–210.
- [26] D. Wakefield, J. Easter, S.N. Breit, P. Clark, R. Penny, *Br. J. Ophthalmol.* 69 (1985) 497–499.
- [27] F.M. Nakhoul, S. Marsh, I. Hochberg, R. Leib, B.P. Miller, A.P. Levy, *JAMA* 284 (2000) 1244–1245.
- [28] T. Chandra, C.N. Lakshmi, T. Padma, M. Vidyavathi, M. Satapathy, *Hum. Hered.* 41 (1991) 347–350.
- [29] R.F. Mullins, S.R. Russell, D.H. Anderson, G.S. Hageman, *FASEB J.* 14 (2000) 835–846.
- [30] A. Hu, Y. Luo, T. Li, X. Guo, X. Ding, X. Zhu, X. Wang, S. Tang, *Graefes Arch. Clin. Exp. Ophthalmol.*, 2012.
- [31] Y. Deguchi, T. Maeno, Y. Saishin, Y. Hori, T. Shiba, M. Takahashi, *Jpn. J. Ophthalmol.* 55 (2011) 128–131.
- [32] M.B. Sasongko, T.Y. Wong, T.T. Nguyen, R. Kawasaki, A. Jenkins, J. Shaw, J.J. Wang, *Diabetes Care* 34 (2011) 474–479.
- [33] S. Kawai, T. Nakajima, S. Hokari, T. Komoda, K. Kawai, *Ann. Clin. Biochem.* 39 (2002) 56–61.
- [34] R.P. Casaroli Marano, K.T. Preissner, S. Vilaro, *Exp. Eye Res.* 60 (1995) 5–17.
- [35] P. Esser, M. Bresgen, M. Weller, K. Heimann, P. Wiedemann, *Graefes Arch. Clin. Exp. Ophthalmol.* 232 (1994) 477–481.
- [36] P.F. Barcelona, J.D. Luna, G.A. Chiabrand, C.P. Juarez, I.A. Bhatt, T. Baba, D.S. McLeod, M.C. Sanchez, G.A. Luty, *Exp. Eye Res.* 91 (2010) 264–272.
- [37] M.C. Sanchez, J.D. Luna, P.F. Barcelona, A.L. Gramajo, P.C. Juarez, C.M. Riera, G.A. Chiabrand, *Exp. Eye Res.* 85 (2007) 644–650.
- [38] R.S. Gray, K. James, J. Merriman, I.R. Starkey, R.A. Elton, B.F. Clarke, L.J. Duncan, *Horm. Metab. Res.* 14 (1982) 389–392.
- [39] F. Wang, J. Yu, Q.H. Qiu, L. Bai, H. Cao, *Zhonghua Yan. Ke. Za Zhi.* 46 (2010) 609–614.
- [40] J.D. Andersen, K.L. Boylan, R. Jemmerson, M.A. Geller, B. Misemer, K.M. Harrington, S. Weivoda, B.A. Witthuhn, P. Argenta, R.I. Vogel, A.P. Skubitz, *J. Ovarian Res.* 3 (2010) 21.
- [41] T. Kakisaka, T. Kondo, T. Okano, K. Fujii, K. Honda, M. Endo, A. Tsuchida, T. Aoki, T. Itoi, F. Moriyasu, T. Yamada, H. Kato, T. Nishimura, S. Todo, S. Hirohashi, *J. Chromatogr. B Anal. Technol. Biomed. Life Sci.* 852 (2007) 257–267.
- [42] Y. Li, Y. Zhang, F. Qiu, Z. Qiu, *Electrophoresis* 32 (2011) 1976–1983.
- [43] B.K. Kim, J.W. Lee, P.J. Park, Y.S. Shin, W.Y. Lee, K.A. Lee, S. Ye, H. Hyun, K.N. Kang, D. Ye, Y. Kim, S.Y. Ohn, D.Y. Noh, C.W. Kim, *Breast Cancer Res.* 11 (2009) R22.
- [44] K. Bijan, A.M. Mlynarek, R.L. Ballys, S. Jie, Y. Xu, M.P. Hier, M.J. Black, M.R. Di Falco, S. LaBoissiere, M.A. Alaoui-Jamali, *J. Proteome Res.* 8 (2009) 2173–2185.
- [45] B. Chatterji, J. Borlak, *Proteomics* 7 (2007) 3980–3991.
- [46] L.M. Brown, S.M. Helmke, S.W. Hunsucker, R.T. Netea-Maier, S.A. Chiang, D.E. Heinz, K.R. Shroyer, M.W. Duncan, B.R. Haugen, *Mol. Carcinog.* 45 (2006) 613–626.
- [47] D. Blanton, Z. Han, L. Bierschenk, M.V. Linga-Reddy, H. Wang, M. Clare-Salzler, M. Haller, D. Schatz, C. Myhr, J.X. She, C. Wasserfall, M. Atkinson, *Diabetes* 60 (2011) 2566–2570.
- [48] K.A. Young, J.K. Snell-Bergeon, R.G. Naik, J.E. Hokanson, D. Tarullo, P.A. Gottlieb, S.K. Garg, M. Rewers, *Diabetes Care* 34 (2011) 454–458.
- [49] H. Dieplinger, D.P. Ankerst, A. Burges, M. Lenhard, A. Lingenhel, L. Fineder, H. Buchner, P. Stieber, *Cancer Epidemiol. Biomarkers Prev.* 18 (2009) 1127–1133.
- [50] D. Jackson, R.A. Craven, R.C. Hutson, I. Graze, P. Lueth, R.P. Tonge, J.L. Hartley, J.A. Nickson, S.J. Rayner, C. Johnston, B. Dieplinger, M. Hubalek, N. Wilkinson, T.J. Perren, S. Kehoe, G.D. Hall, G. Daxenbichler, H. Dieplinger, P.J. Selby, R.E. Banks, *Clin. Cancer Res.* 13 (2007) 7370–7379.
- [51] D.H. Jeong, H.K. Kim, A.E. Prince, D.S. Lee, Y.N. Kim, J. Han, K.T. Kim, *J. Gynecol. Oncol.* 19 (2008) 173–180.
- [52] N. Walsh, P. Dowling, N. O'Donovan, M. Henry, P. Meleady, M. Clynes, J. Proteomics 7 (2008) 561–571.
- [53] M. Sanchez-Carbayo, N.D. Succi, L. Richstone, M. Corton, N. Behrendt, J. Wulffuhle, B. Bochner, E. Petricoin, C. Cordon-Cardo, *Am. J. Pathol.* 171 (2007) 1650–1658.
- [54] J. Yang, N. Ramnath, K.B. Moysich, H.L. Asch, H. Swede, S.J. Alrawi, J. Huberman, J. Geradts, J.S. Brooks, D. Tan, *BMC Cancer* 6 (2006) 203.
- [55] M. Habeck, *Mol. Med. Today* 5 (1999) 503.
- [56] R.C. Koya, H. Fujita, S. Shimizu, M. Ohtsu, M. Takimoto, Y. Tsujimoto, N. Kuzumaki, *J. Biol. Chem.* 275 (2000) 15343–15349.
- [57] D.S. Dalpathado, H. Desaire, *Analyst* 133 (2008) 731–738.
- [58] T. Rabilloud, M. Heller, F. Gasnier, S. Luche, C. Rey, R. Aebbersold, M. Benahmed, P. Louisot, J. Lunardi, *J. Biol. Chem.* 277 (2002) 19396–19401.
- [59] E. Wagner, S. Luche, L. Penna, M. Chevallet, A. van Dorselaer, E. Leize-Wagner, T. Rabilloud, *Biochem. J.* 366 (2002) 777–785.
- [60] H.L. Chan, P.R. Gaffney, M.D. Waterfield, H. Anderle, M.H. Peter, H.P. Schwarz, P.L. Turecek, J.F. Timms, *FEBS Lett.* 580 (2006) 3229–3236.
- [61] H.C. Chou, Y.C. Lu, C.S. Cheng, Y.W. Chen, P.C. Lyu, C.W. Lin, J.F. Timms, H.L. Chan, *J. Proteomics* 75 (2012) 3158–3176.
- [62] C.L. Wu, H.C. Chou, C.S. Cheng, J.M. Li, S.T. Lin, Y.W. Chen, H.L. Chan, *J. Proteomics* 75 (2012) 1991–2014.